PAPER • **OPEN ACCESS**

Response surface methodological (RSM) approach for optimizing the mechanical properties of starch-based films incorporated with chitosan-encapsulated thymol

Physica Scripta

PAPER

Response surface methodological (RSM) approach for optimizing the mechanical properties of starch-based films incorporated with chitosan-encapsulated thymol

Ruzanna Ahmad Shapi'i[1,2], **Siti Hajar Othman**[1,2,*], **Mohd Nazli Naim**[2], **Intan Syafinaz Mohamed Amin Tawakkal**[2] **and Mohd Salahuddin Mohd Basri**[2]

[1] Institute of Nanoscience and Nanotechnology, Universiti Putra Malaysia, 43400 Serdang, Selangor, Malaysia
[2] Department of Process and Food Engineering, Faculty of Engineering, Universiti Putra Malaysia, 43400 UPM Serdang, Selangor, Malaysia
[*] Author to whom any correspondence should be addressed.

E-mail: ruzannashapii91@gmail.com, s.hajar@upm.edu.my, mohdnazli@upm.edu.my, intanamin@upm.edu.my and salahuddin@upm.edu.my

Keywords: additives, biomaterial, blend, casting, film, packaging

Supplementary material for this article is available online

OPEN ACCESS

RECEIVED
15 May 2025

REVISED
9 August 2025

ACCEPTED FOR PUBLICATION
3 September 2025

PUBLISHED
15 September 2025

Abstract

In this study, starch-based films incorporated with glycerol and chitosan-encapsulated thymol (CNP-T) were formulated for potential active packaging applications. The central composite design (CCD) technique was used to formulate the films and 42 runs were generated based on three replications on two factors at five levels, particularly the concentration of glycerol (V1: 0, 6.25, 12.5, 18.75, 25% wt/wt of starch) and concentration of CNP-T (V2: 0, 0.2, 0.4, 0.6, 0.8% wt/v of starch). The optimized values for V1 and V2 were found to be 25% wt/wt and 0.8% wt/v, respectively, whereby the predicted values of the tensile strength (TS) and elongation at break (EAB) were 17.40 MPa and 40.01%, respectively. The optimized formulation offers a promising foundation for producing starch-based films containing CNP-T with enhanced mechanical properties, suitable for sustainable active packaging applications in the food industry.

1. Introduction

Nowadays, the development of active biopolymer packaging films serving as an alternative to fossil-based packaging films which are not environmentally friendly and sustainable. Among the many biopolymers that can be utilized to produce biodegradable packaging films, starch is easily obtained from abundant sources (cassava, corn, potato, sweet potato, wheat), non-toxic, relatively easy to handle, naturally biodegradable, and cheap [1]. Moreover, the production of thin films from starch does not require synthetic chemicals thus resulting in non-toxic and safe films for use as food-packaging materials [2]. In terms of applications, it is vital to ensure that starch-based films exhibit good mechanical strength, thus the packaged food can withstand stress during handling, storage, and transportation. Starch-based films are usually known to be brittle and require the incorporation of plasticizers to improve flexibility. Glycerol is widely used as a plasticizer due to its non-toxic, environmentally friendly nature, and compatibility with amylose in starch [3]. It interrupts the packing of the amylose chain and forms hydrogen bonds with starch molecules, thereby reducing intermolecular attraction and allowing greater chain mobility. This results in a less dense matrix under tensile stress and improves the flexibility and pliability of films [4]. Several studies have reported that incorporating 20%–30% wt/v of glycerol is effective in plasticizing starch-based films [2, 4, 5].

The incorporation of other components, such as nano-sized fillers or nanofillers (ranging from 1 to 100 nm), can also improve the mechanical properties and other properties of biopolymer films, including barriers and thermal properties [6]. The improvement of film properties is attributed to the effectiveness of the nanoscale size that provides a large surface area for intermolecular interaction between filler and matrix, thus

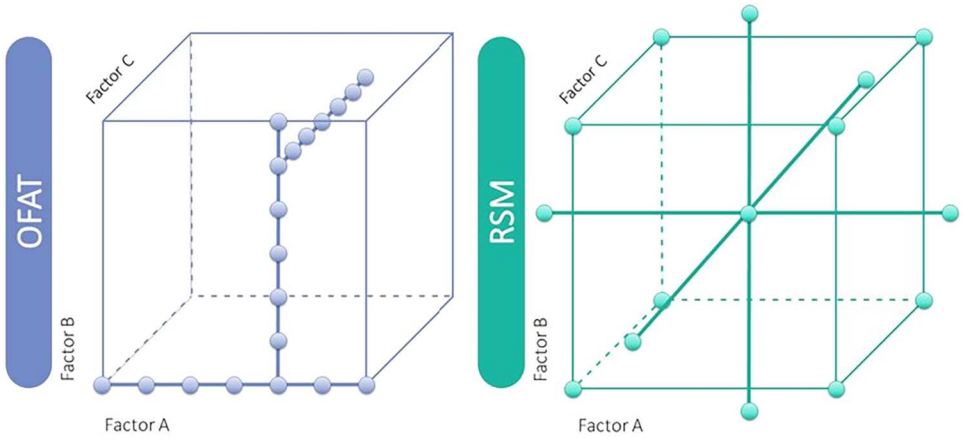

Figure 1. Experiment design space explored by OFAT and RSM (CCD) approach. Reproduced from [25]. CC BY 3.0.

enhancing the properties of biopolymers [7]. Some nanofillers also exhibit antimicrobial and antioxidant properties, making them valuable for food packaging applications. For example, the incorporation of chitosan nanoparticles (CNP), zinc oxide nanoparticles (ZnO) [8], and silver nanoparticles [9] into the biopolymer matrix exhibited antimicrobial properties that can maintain food quality [10]. Moreover, a few studies also reported on the addition of nano-sized active compounds, such as oregano essential oil, cinnamomum essential oil, eugenol, thymol, either encapsulated or in emulsion form, into biopolymer films to enhance their functional properties as active packaging materials [11–15]. Despite the benefits of nanofillers, it is very crucial to ensure the well-dispersion of nanofillers and good intermolecular interaction between filler-matrix, which could influence the mechanical properties of the films [16]. Additionally, the hydrophobic nature of EO also potentially leads to poor compatibility with hydrophilic biopolymer matrices, thus resulting in non-homogeneous films and weak mechanical strength [5].

Thymol, a bioactive compound found predominantly in thyme (*Thymus vulgaris*) and oregano (*Origanum vulgare*), is widely used as an antibacterial agent in many products, including mouthwash, topical ointment, balms, and toothpaste [17]. Thymol is well known for its great antibacterial activity against both Gram-positive and Gram-negative bacteria [18]. Encapsulation of thymol in CNP (CNP-T) not only enhances their functional properties, such as antioxidants and antimicrobial properties, but also improves the compatibility of thymol with hydrophilic starch matrix, thus promising to improve the films' mechanical properties [19]. However, to the best of our knowledge, no study has reported the incorporation of CNP-T into starch-based films. Previous studies by Medina *et al* [20] and Caro *et al* [21] incorporated CNP-T into quinoa protein films via solvent casting and thermal ink-jet printing, respectively. Medina *et al* [20] found that adding 1% CNP-T slightly improved film strength and water barrier properties, whereas Caro *et al* [21] observed no enhancement in tensile strength and only minor improvements in water resistance. These inconsistencies may result from the differences in size, stability, and concentration of CNP-T within the films. Noting that Caro *et al* [21] used glycerol as a plasticizer at fixed amounts of 20 and 30% while Medina *et al* [20] did not use any plasticizer. Although both studies demonstrated strong antibacterial activity of starch/CNP-T films, there is still uncertainty on the relationship between plasticizer and CNP-T addition with the mechanical properties of starch-based films. Therefore, further investigation is needed to understand the interactions between CNP-T and the biopolymer matrix, which could provide valuable insights for developing active biopolymer films.

Different amount or types of filler, plasticizer, biopolymer matrix, and others may exhibited different trend of mechanical properties of the films [22, 23]. Many previous studies in this field have relied on the resource-intensive approach known as one-factor-at-time (OFAT). It is crucial to use a statistical analysis and regression coefficient model to determine the ideal composition of biopolymer films. On the other hand, the response surface methodology (RSM) provides many advantages including cost-efficiency as it can reduce the number of experiments, manpower, and materials used. Among the series of RSM models available, CCD is widely utilized to investigate main effects, interactions, and optimization studies [24]. As shown in figure 1, CCD enables accurate estimation of main effects and their interactions while simultaneously analyzing multiple factors, but it is limited for OFAT. By incorporating CCD as part of experimental design, researchers can efficiently determine the optimal composition of biopolymer films, leading to improved efficiency and cost-effectiveness in the manufacturing process.

Several previous works have successfully using CCD to optimize the starch-based film formulation, including taro peel starch films with glycerol [26], pearl millet starch films with carrageenan gum [27], potato

Table 1. Factors and levels used for the optimization.

Factor	Unit	Notation	Level				
			−2	−1	0	1	2
Concentration of glycerol	% wt/wt	V1	0	6.25	12.5	18.75	25
Concentration of CNP-T	% wt/v	V2	0	0.2	0.4	0.6	0.8

starch with gelatin [28], mango kernel starch with chitosan [29], and rice starch with nut shell powder [30], resulting in improvement of mechanical and barrier properties. However, to the best of our knowledge, no previous work has used CCD or other RSM models for optimizing the formulation of glycerol and CNP-T in starch-based film. Therefore, the aim of this study is to evaluate the main and interaction effects of glycerol (V1) and CNP-T (V2) concentrations on the tensile strength (TS) and elongation at break (EAB) of starch-based films using a CCD. This study also aims to predict and validate the optimal concentrations of V1 and V2 for producing starch-based films with desirable mechanical properties. This work may provide insight into the development of starch-based materials with improved mechanical performance for promising applications as active food packaging.

2. Materials and methods

2.1. Experimental design

The experimental design using CCD was performed in the Minitab Software (Minitab Inc., State College, Pa., USA). The experiment was designed based on two factors, namely the concentration of glycerol (V1) and the concentration of CNP-T (V2) at five levels as tabulated in table 1. The parameters for other factors such as concentration of starch and gelatinization temperature were fixed. TS and EAB were appointed as responses.

The experiment consisted of five levels, two factors, and two responses, with a total of 42 samples, including three replicates for each formulation. The total block value was set to 1 and the analysis was conducted in a randomized order to avoid any bias. Table 2 presents the completed CCD, including both coded and uncoded levels of the factors.

To assess the impact of each factor and their interactions on the mechanical properties, an analysis of variance (ANOVA) was conducted using a significance level of 95% and a p-value of 0.05. The experimental data were fitted to a second-order polynomial model to obtain the regression coefficient model. Equation (1) presents the model used for response surface analysis [24].

$$y = \beta_0 + \sum_{t=1}^{3} \beta_i X_i + \sum_{i}^{3} \beta_{ii} X_i^2 + \sum_{i-1}^{2} \sum_{j=i+1}^{3} \beta_{ij} X_i X_j \quad (1)$$

where y is the response, β_0, β_i, β_{ii}, and β_{ij} are regression coefficients for the intercept, linear, quadratic, and interaction terms, respectively. X_i and X_j are coded values for the independent variables.

The mathematical model that is developed by ANOVA was used for optimization purposes, by basing on the value of the correlation coefficient, R^2. The mechanical properties of commercial plastic, low-density polyethylene (LDPE) were set as the target goal during the optimization, whereby the TS and EAB values are 16.2 MPa and 68.7%, respectively [31]. The reason LDPE was chosen as a target goal is because LDPE exhibits the behavior of flexible material which is widely used as food packaging materials.

2.2. Raw materials

Chitosan (low molecular weight: 50 kDa, viscosity: 20–300 cP in 1% wt/v of acetic acid, deacetylation: 75%–85%) and sodium tripolyphosphate (TPP) were obtained from Sigma-Aldrich, USA. Acetic acid, sodium hydroxide (NaOH), tapioca starch, glycerol, and magnesium nitrate ($MgNO_3$) were purchased from R&M Chemicals, UK. All chemicals used in this study were of analytical grade.

2.3. CNP-T preparation

CNP-T suspension was produced by encapsulating the thymol into chitosan nanoparticles via the ionic gelation technique according to the formulation of CNP-T produced by Shapi'i *et al* [32]. The chitosan-to-thymol ratio was fixed at 1:0.5 (w/w) throughout the preparation of CNP-T.

The morphology of the CNP-T was analyzed using transmission electron microscopy (TEM) (JEM-2100, JEOL, Japan). One drop of the dispersion containing CNP-T was deposited on a carbon grid and left to dry under ambient conditions (20 °C) for at least 30 min before viewing by TEM. The images of CNP-T distribution with x10 k magnifications were captured with an accelerating voltage of 200 kV.

Table 2. Design matrix.

Sample	Coded factor		Uncoded factor	
	V1	V2	V1	V2
S1	2	0	25	0.4
S2	0	2	12.5	0.8
S3	0	−2	12.5	0
S4	0	−2	12.5	0
S5	0	2	12.5	0.8
S6	0	0	12.5	0.4
S7	−2	0	0	0.4
S8	0	0	12.5	0.4
S9	0	0	12.5	0.4
S10	0	−2	12.5	0
S11	0	0	12.5	0.4
S12	0	0	12.5	0.4
S13	2	0	25	0.4
S14	0	0	12.5	0.4
S15	0	0	12.5	0.4
S16	0	0	12.5	0.4
S17	0	0	12.5	0.4
S18	−2	0	0	0.4
S19	2	0	25	0.4
S20	0	2	12.5	0.8
S21	−2	0	0	0.4
S22	−1	−1	6.25	0.2
S23	0	0	12.5	0.4
S24	1	−1	18.75	0.2
S25	−1	−1	6.25	0.2
S26	−1	1	6.25	0.6
S27	0	0	12.5	0.4
S28	1	1	18.75	0.6
S29	1	−1	18.75	0.2
S30	1	−1	18.75	0.2
S31	0	0	12.5	0.4
S32	0	0	12.5	0.4
S33	0	0	12.5	0.4
S34	0	0	12.5	0.4
S35	1	1	18.75	0.6
S36	0	0	12.5	0.4
S37	−1	1	6.25	0.6
S38	0	0	12.5	0.4
S39	1	1	18.75	0.6
S40	0	0	12.5	0.4
S41	−1	1	6.25	0.6
S42	−1	−1	6.25	0.2

2.4. Films preparation

CNP-T was incorporated into the starch film-forming solution according to the formulation of V1 and V2 as generated by the CCD. Film preparation followed the method of Shapi'i *et al* [33], with some modifications whereby the amount of tapioca starch in the solvent, which was distilled water, was fixed at 5% wt/v. The film-forming solutions were cast into the polystyrene petri dish and then left to dry in the air-conditioned room (20 °C) on a flat table for 48 h, as illustrated in figure 2(a). Film thickness was measured at five random points using a digital micrometer (Mitutoyo, Japan), and the average thickness (0.098 mm) was used to calculate the TS and EAB.

2.5. Mechanical properties analysis

Mechanical testing was performed to determine TS and EAB using a texture analyzer (TA.XT2 Stable Micro Systems, UK) following the ASTM D882 standard [34]. Film strips (100 mm × 15 mm) were placed between the grips as shown in figure(b), with an initial grip separation of 60 mm and a test speed of 0.5 mm/s.

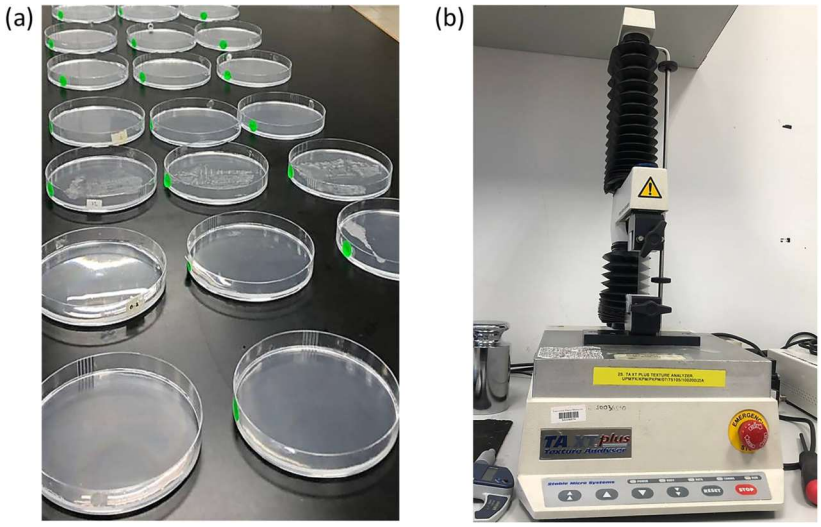

Figure 2. (a) Films preparation via solvent casting, (b) Mechanical properties analysis.

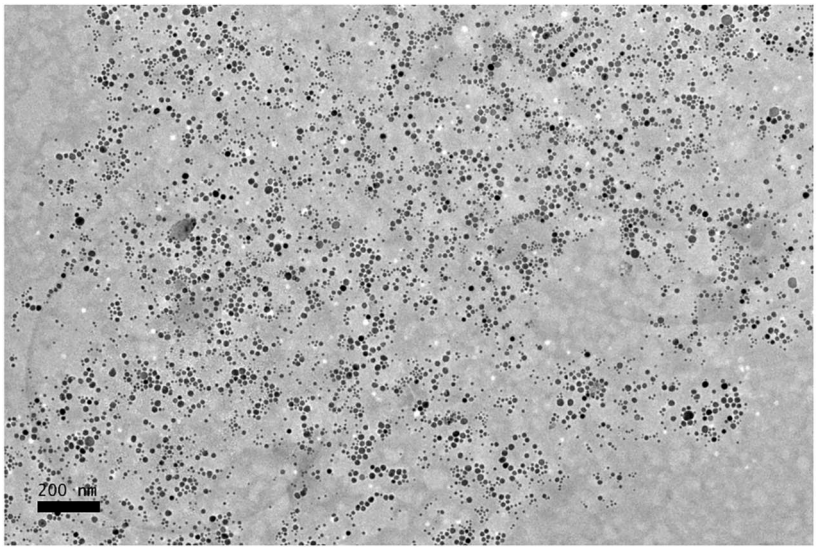

Figure 3. TEM image of CNP-T at a magnification of ×10 k.

3. Results and discussion

3.1. CNP-T

The TEM image of synthesized CNP-T (figure 3) shows well-dispersed, spherical nanoparticles with no visible agglomeration. ImageJ software measured an average size of approximately 10 nm of the CNP-T. The well dispersion, small, and uniform size distribution of CNP-T can enhance their compatibility with starch, thus promoting good dispersion of CNP-T within the films.

In addition, the physicochemical properties of the synthesized CNP-T have been characterized in our previous study [32]. The nanoparticles exhibited a hydrodynamic diameter of 57.17 ± 0.75 nm, a polydispersity index (PDI) of 0.237 ± 0.013, and a zeta potential of $+50.30 \pm 0.25$ mV, indicating a narrow size distribution and good colloidal stability. The encapsulation efficiency (EE) and loading capacity (LC) were found to be 57.53% and 41.52%, respectively, suggesting that more than half of the initial thymol was successfully entrapped within the chitosan matrix, with a relatively high amount of thymol loaded per nanoparticle mass. These characteristics are favorable for maintaining dispersion stability and ensuring effective delivery of thymol within the film matrix.

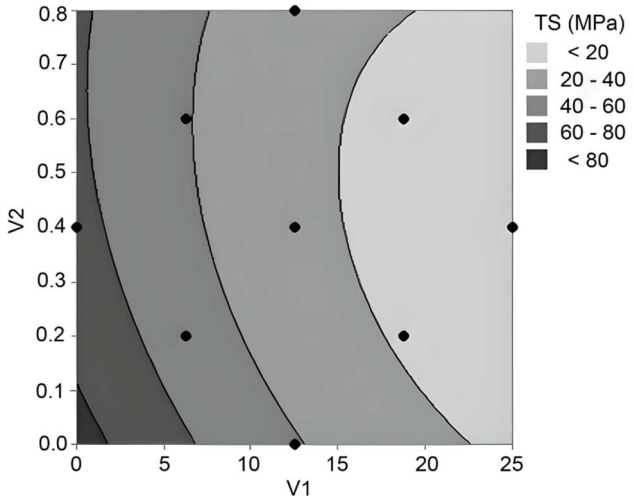

Figure 4. Contour plot of V2 versus V1 for TS; V1: glycerol concentration, V2: CNP-T concentration.

Table 3. ANOVA table for TS.

Term	Term	Coefficient	Standard error	p
Constant		88.39	1.20	0
Concentration of glycerol	V1	−4.616	0.871	0.000
Concentration of CNP-T	V2	1.259	−3.52	0.001
Concentration of glycerol*Concentration of glycerol	V1*V1	0.0704	0.639	0.000
Concentration of CNP-T*Concentration of CNP-T	V2*V2	0.01517	0.639	0.001
Concentration of glycerol*Concentration of CNP-T	V1*V2	0.0203	1.51	0.300

$R^2 = 0.9027$, R^2 (adj) = 0.8860

3.2. Effect of V1 and V2 on the TS

From the ANOVA (table 3), the linear terms of V1 and V2 are highly significant, at p-values of 0.000 and 0.001, respectively. The squared terms for both V1*V1 and V2*V2 are also highly significant at p-values of 0.000 and 0.001, respectively. However, V1*V2 shows a p-value of 0.3 which is not significant (0.005) to the TS, thus there is no significant relationship between V1 and V2 towards TS.

The R^2 is 0.9027 which is near to 1, depicting that the model equation can predict the optimum value of TS with high accuracy. The significant ($p < 0.005$) squared term of V1*V1 and V2*V2, indicates that the relationship between both factors and TS obeys the quadratic function [24]. The highest absolute coefficient value is V1 which is 4.616, thus indicating the greatest effect of glycerol concentration on the response. The model equation for the TS of films is given in equation (2):

$$TS = 88.39 - 4.616(V1) - 1.259(V2) + 0.0704(V1)^2 + 0.01517(V2)^2 + 0.0203(V1)(V2) \quad (2)$$

where TS represents the tensile strength while V1 and V2 are the concentration of glycerol and concentration of CNP-T, respectively. This regression coefficient model was employed to construct the contour plot of V1 against V2 against TS.

Figure 4 shows the contour plot of the effect of V1 and V2 on the TS of films developed using equation (2). It can be observed that the TS of the films decreased with the increase in V1. For example, at V2 = 0%, TS decreased from the range greater than 80 MPa to 60–80 MPa, from 60–80 MPa to 40–60 MPa, from 40–60 MPa to 20–40 MPa, and from 20–40 MPa to less than 20 MPa when V1 was increased from 0 to 5%, 5 to 10%, 10 to 15%, and 15 to 25%, respectively. The same pattern was observed for other V2 values of 0.1, 0.2, 0.3, 0.4, 0.5, 0.6, 0.7, and 0.8% wt/v. It is worth noting that the TS values greater than 80 MPa seemed unrealistic for starch-based films. Indeed, the values were not obtained experimentally but were only part of the RSM-generated contour plot (figure 4), which displays predicted values across the full design space. These high TS values occurred at combinations of low or zero plasticizer content with high CNP-T content, which would result in extremely brittle films that are unsuitable for packaging applications.

Based on these observations, it can be concluded that there is a clear inverse relationship between V1 and the tensile strength of the material, regardless of the value of V2. Mali *et al* [35] via the OFAT approach reported

Table 4. ANOVA table for EAB.

Term	Notation	Coefficient	Standard error	p
Constant		7.58	**1.51**	**0.329**
Concentration of glycerol	V1	−2.691	1.10	0.000
Concentration of CNP-T	V2	0.192	1.10	0.950
Concentration of glycerol*Concentration of glycerol	V1*V1	0.1598	0.809	0.000
Concentration of CNP-T*Concentration of CNP-T	V2*V2	−0.00436	0.809	0.405
Concentration of glycerol*Concentration of CNP-T	V1*V2	0.0017	1.91	0.947

$R^2 = 0.8010$, R^2 (adj) $= 0.7669$

a similar trend of the effect of glycerol at the concentration between 0 to 40% wt/wt on tapioca, corn, as well as yam starch films. They found that despite the types of starch, higher concentrations of glycerol enhanced the EAB but reduced the TS. The TS of starch films decreased from 7.12 to 1.12 MPa ($p < 0.05$) when the glycerol concentration was increased from 10 to 25% as reported by Shapi'i *et al* [36]. This pattern was found owing to the increased amount of glycerol used in the starch-based films which led to the higher interruption of glycerol molecules leading to the formation of more empty spaces within the matrix of starch. The empty spaces formation in the starch matrix lowered the forces of intermolecular attraction in amylose and amylopectin, therefore it produces films that are malleable and pliable.

From figure 4, when V1 = 0, 5, 10, 15, 20, 25% wt/wt and V2 was increased from 0 to 0.8% wt/v, the TS decreased from the range of >80 MPa to 0–20 MPa. It can be presumed that there was a decrement in the TS of films when V2 was increased at any value of V1. It is worth noting that other studies that used the OFAT approach also reported similar trends of TS when nanoencapsulated essential oil was incorporated into biopolymer films. Medina *et al* [20] reported a decrement trend of TS from 6.9 to 6.3 MPa when 2.5% wt/v of CNP-T was added to the quinoa films. Previously, Mohsenabadi *et al* [37] found that increasing the CN-REO content in the starch-CMC films from 0.00125 to 0.0025% wt/v enhanced the TS but increasing the CN-REO (0.00375% wt/v) further lowered the TS. The reduction in TS may be due to the agglomeration of nanoparticles in the matrix of film, which reduced TS due to the film structure heterogeneity [2].

Moreover, the presence of free thymol in the starch matrix can lead to the destabilization of film structure due to the different hydrophilicity/hydrophobicity behaviors of different materials, thus reducing the TS of films. As reported by Cruz-Tirado *et al* [38] who produced sweet potato starch-based foam incorporated with non-encapsulated oregano or thyme oil, the presence of oil in the starch matrix can interrupt the amylose, amylopectin-amylopectin, or amylose-amylopectin interactions. In this work, thymol tends to be released from CNP-T as the CNP-T was dispersed in water before being mixed into the gelatinized starch solution. As thymol has a hydroxyl group, the presence of water will facilitate thymol to be adsorbed onto the surface of CNP-T, thus interfering with the starch matrix [39].

3.3. Effect of V1 and V2 on the EAB

The results of the ANOVA of EAB are depicted in table 4. The outcomes demonstrate that both V1 and V1*V1 are highly significant whereby the p-value is 0.000. Meanwhile, both V2 and V2*V2 are non-significant at p-values of 0.905 and 0.405, respectively. The p-value of V1*V2 is 0.947 which is non-significant (>0.005) to the EAB, thus there is no relationship between V1 and V2 towards EAB.

The R^2 is 0.8010, which shows that 80.10% of the sample variation in the EAB was related to the factors V1 and V2. The R^2 value for EAB was slightly lower than the R^2 value for TS (0.9027), due to the behavior of EAB that is more sensitive to surrounding conditions and factors not included in the model, such as film thickness, relative humidity, temperature, and moisture content [40]. On the other hand, V1 has the greatest impact on the response, because of the highest absolute coefficient value of 2.691. The V1*V1 which is significant ($p < 0.005$), shows that the relationship between the factors and response obeys the quadratic function [24]. The model equation for the EAB of films is given in equation (3):

$$\begin{aligned} \text{EAB} = 7.58 &- 2.691(\text{V1}) + 0.192(\text{V2}) + 0.1598(\text{V1})^2 \\ &- 0.00436(\text{V2})^2 + 0.0017(\text{V1})(\text{V2}) \end{aligned} \tag{3}$$

where EAB represents the elongation at break while V1 and V2 are the concentration of glycerol and the concentration of CNP-T, respectively. This regression coefficient model was employed to construct the contour plot of V1 against V2 against the EAB of the films.

Figure 5 shows a contour plot of the effect of V1 and V2 on the EAB of films developed using equation (3). It can be observed in the contour plot that EAB increased when V1 was increased from 0 to 25% wt/wt at any V2. When V1 is between 0 to 15%, the EAB values fall in the range of 0 to 10% which indicates that the films

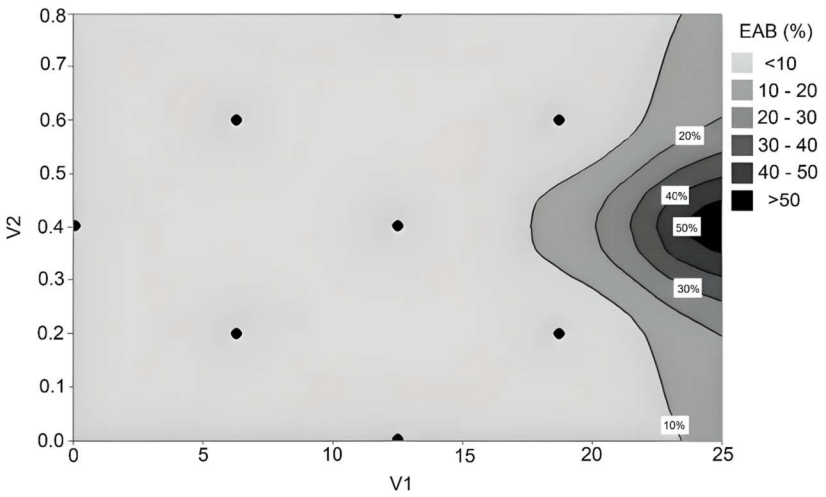

Figure 5. Contour plot of V2 versus V1 for EAB; V1: glycerol concentration, V2: CNP-T concentration.

produced were brittle [41]. When V1 is between 15 to 25%, the EAB increased from the range of less than 10% to the range of more than 50% which indicates that the films became more flexible when glycerol was increased. A similar pattern was found by Shapi'i *et al* [36], whereby the EAB enhanced from 1.89 to 67% (improved 34-fold) with the increment in glycerol concentrations from 10 to 25% wt/wt in starch films, respectively. This outcome showed that the starch films' EAB was greatly dependent on the glycerol concentration ($p < 0.05$). The increment in the starch films' EAB with the increase in the glycerol concentration was because of the free volume formation formed by glycerol molecules interrupting the starch chain. When external stress is applied, the starch chains can move easily and tolerate stress, thereby enhancing the EAB of the films. This phenomenon led to an increase in elasticity and flexibility but decreased the strength of the films.

At lower levels of V1 (0 to 15%), V2 has an insignificant effect on the EAB of the films. At V1 = 20%, increasing V2 from 0 to 0.4% improved the EAB of the films, but further increasing V2 to 0.8% reduced the EAB. At V1 = 25%, increasing V2 from 0 to 0.4% significantly enhanced the EAB of the films, but increasing V2 beyond 0.4% decreased the EAB. These findings highlight that the effect of V2 on EAB is dependent on the level of V1.

Medina *et al* [20] reported that there was a slight increase from 36.9 to 40.2% in the EAB of quinoa film produced without the addition of plasticizer when 1% wt/v of CNP-T was added to the films. Meanwhile, a further increment in the concentration of CNP-T to 2.5% wt/v slightly enhanced the films' EAB to 33.2%. A similar trend of finding was reported by Mohsenabadi *et al* [37], who varied the concentration of CN-REO in the starch-CMC films produced with the addition of 60% wt/wt of glycerol (per dry weight of starch). They found that the increase of CN-REO from 0.00125 to 0.0025% wt/v, increased the EAB of the starch-CMC films from 140.83 to 151.45%, whereby the increment of EAB was about 10.62%. Further augmented the CN-REO amount (0.00375% wt/v) in the starch-CMC films led to the decrease of EAB (85.57%). Based on the findings in this study and in the previous studies, it can be deduced that the incorporation of encapsulated EO in biopolymer films has only small effects on the EAB values (small changes of EAB values).

3.4. Optimization

Optimization is conducted to gain the best combination of glycerol concentration and CNP-T concentration in producing films with good mechanical properties. The targeted mechanical properties of the films were determined based on the TS and EAB values of commercial flexible films, LDPE (16.2 MPa and 68.7%, respectively). Figure 6 shows the optimization results. The values of V1 and V2 were 25% wt/wt and 0.8%, wt/v respectively, whereby the predicted values of TS and EAB were 17.4133 MPa and 40.949%, respectively. Composite desirability (D) was used to assess the overall optimization of the responses. It is worth noting that the desirability value ranges from zero to one, whereby the value close to one represents that the multiple responses are close to the targeted values [27]. In this work, the D value was 0.7566, which indicates that the optimized factors can produce films that exhibit TS and EAB, which are moderately close to the targeted values (TS and EAB of LDPE). The individual desirability (d) in figure 6 for each predicted response was then used to understand how close the individual predicted response was to the target response [42]. It is important to highlight that d value in figure 3 for TS was 0.9729, which indicates that the optimization was still effective in achieving a formulation that meets the target TS value. The lower of the overall desirability value was mainly

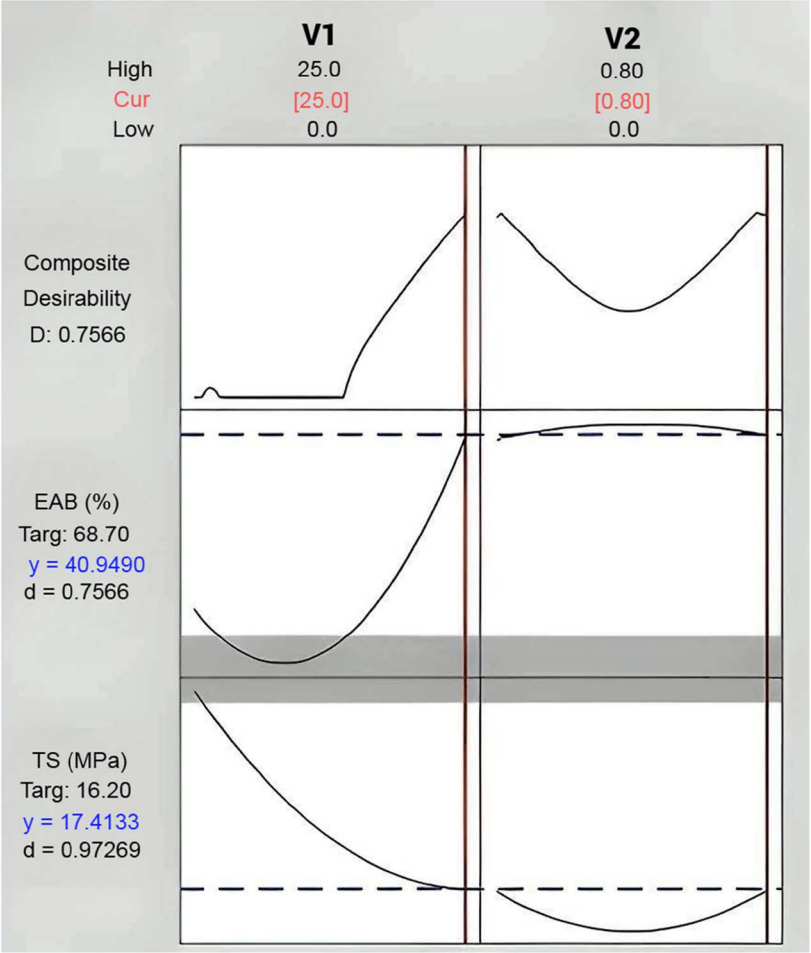

Figure 6. Optimization of V1 and V2; V1: glycerol concentration, V2: CNP-T concentration.

Table 5. Predicted and experimental responses of the films.

Response	Predicted value[a]	Experimental value (N = 3)[b, d]	Absolute residual error (%)[c]
TS	17.41	12.33 ± 0.40	29
EAB	40.95	28.25 ± 0.61	31

[a] Predicted values obtained from the model equations.
[b] Experimental values obtained for the starch-based film prepared using the optimal film formulation.
[c] Absolute residual error (%) = [(experimental value-predicted value)/predicted value] × 100
[d] N represents the number of samples.

influenced by the lower desirability value of EAB (0.5885), which could be due to the insufficient glycerol amount within the tested range to achieve the targeted EAB value. The higher concentration of glycerol (>25%) may be required to increase EAB value, but this could decrease the TS of films.

The validation of the RSM model was conducted by preparing starch/CNP-T films using the optimized formulation (25% wt/wt glycerol and 0.8% wt/v CNP-T). As tabulated in table 5, the experimental values of TS and EAB obtained from the experiment were 12.33 ± 0.40 MPa and 28.25 ± 0.61%, respectively. Comparing the experimental value of TS and EAB with the predicted value of TS (17.41 MPa) and EAB (41.95%), the absolute residual error is 29% and 31%, respectively. The deviation may be attributed to factors such as variation in film thickness, possible thymol volatilization, or heterogeneity in dispersion of CNP-T within the starch matrix. Despite this discrepancy, the experimental results aligned with the trend predicted by the model, confirming the significant influence of glycerol and CNP-T on the mechanical performance of the films.

3.5. Contour plots superimposition

Both contour plots of the TS and EAB were combined to plot the superimposed graphs. This method is superior to the classical OFAT method, which is lacking in the interaction of variables. Figure 7 shows the representation

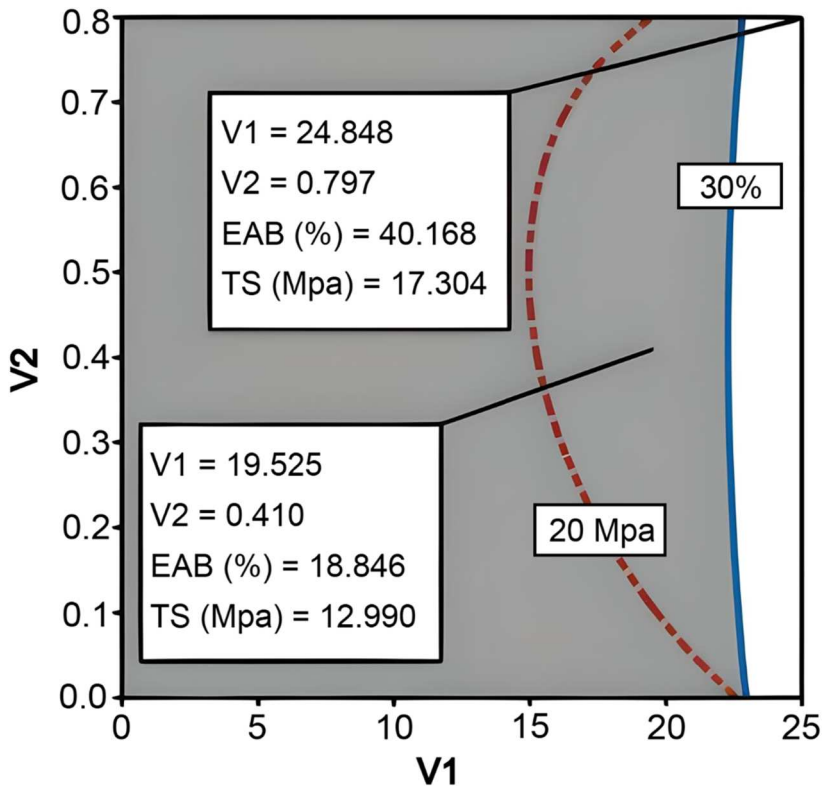

Figure 7. Superimposed contour plots of TS and EAB; V1: glycerol concentration, V2: CNP-T concentration.

of the optimum range of concentration of glycerol and concentration of CNP-T for the formulation of the films. The dash and solid lines represent the contour line for TS and EAB, respectively. As shown on the superimposed contour plots, the optimum ranges of V1 and V2 for the acceptable TS and EAB (represented by unshaded region) were found to be 23%–25% and 0%–0.8%, respectively. The superimposed contour plots can be used as a reference template to predict the responses produced by any values of V1 and V2 within the range. For example, figure 7 shows that the expected TS and EAB for V1 = 24.848% and V2 = 0.797%, which falls in the acceptable range, will be at 17.304 MPa and 40.168%, respectively. Meanwhile, the expected TS and EAB for V1 = 19.525% and V2 = 0.410%, which falls outside the accepted range, will be at 12.990 MPa and 18.846%, respectively.

4. Conclusions

The present work addresses a research gap, as no prior work has employed CCD or any other RSM to investigate the interaction effects of glycerol and CNP-T concentrations on the mechanical properties of starch films. Regression modelling revealed the significant effect of the V1 on the mechanical properties (TS and EAB) of starch/CNP-T films. Meanwhile, V2 only has a significant effect on the TS and an insignificant effect on the EAB of the films. This study managed to formulate the starch/CNP-T films that resulted in the optimized values of TS and EAB films that are comparable by 75% with the commercial LDPE. Extended research into the other parameters such as the amount of starch, film thickness, drying temperature, pH, and storage conditions that affect the properties of starch/CNP-T films should be pursued to ensure the accurate formulation and effective application of the produced starch/CNP-T films. Furthermore, the effect of the parameters on the barrier and bioactivity properties of the starch/CNP-T films should also be explored experimentally and via RSM to assess the full potential for active packaging applications. Evaluating water vapor permeability and oxygen transmission rate will be essential for determining the effectiveness of the films in protecting moisture and oxygen-sensitive products. The incorporation of CNP-T is expected to provide synergy in the antibacterial properties of chitosan and thymol, which should be validated against the foodborne pathogens. Overall, balanced integration of mechanical properties, barrier properties, and bioactive functionality should be taken into account in future studies to produce effective active food packaging.

Acknowledgments

This work was supported by the Ministry of Higher Education under Fundamental Research Grant Scheme (FRGS/1/2024/TK05/UPM/02/9).

Data availability statement

All data that support the findings of this study are included within the article (and any supplementary files).

Author contributions

Ruzanna Ahmad Shapi'i
Conceptualization (equal), Data curation (equal), Formal analysis (equal), Investigation (equal), Methodology (lead), Visualization (lead), Writing – original draft (lead)

Siti Hajar Othman 0000-0002-0922-1323
Conceptualization (equal), Data curation (equal), Formal analysis (equal), Funding acquisition (lead), Investigation (equal), Project administration (lead), Supervision (lead), Validation (equal), Visualization (supporting), Writing – review & editing (lead)

Mohd Nazli Naim
Supervision (equal), Validation (equal)

Intan Syafinaz Mohamed Amin Tawakkal 0000-0003-2796-2608
Supervision (equal), Validation (equal)

Mohd Salahuddin Mohd Basri
Supervision (equal), Validation (equal)

References

[1] Rivadeneira-Velasco K E, Utreras-Silva C A, Díaz-Barrios A, Sommer-Márquez A E, Tafur J P and Michell R M 2021 Green nanocomposites based on thermoplastic starch: a review *Polymers (Basel)* **13** 1–36
[2] Shapii R A, Othman S H, Basha R K and Naim M N 2022 Mechanical, thermal, and barrier properties of starch films incorporated with chitosan nanoparticles *Nanotechnol Rev.* **11** 1464–77
[3] Basiak E, Lenart A and Debeaufort F 2018 How glycerol and water contents affect the structural and functional properties of starch-based edible films *Polymers (Basel)* **10** 1–18
[4] Tarique J, Sapuan S M and Khalina A 2021 Effect of glycerol plasticizer loading on the physical, mechanical, thermal, and barrier properties of arrowroot (Maranta arundinacea) starch biopolymers *Sci. Rep.* **11** 1–17
[5] Nordin N, Othman S H, Rashid S A and Basha R K 2020 Effects of glycerol and thymol on physical, mechanical, and thermal properties of corn starch films *Food Hydrocoll* **106** 105884
[6] Muñoz-Gimena P F, Oliver-Cuenca V, Peponi L and López D 2023 A review on reinforcements and additives in starch-based composites for food packaging *Polymers (Basel)* **15** (13) 1–45
[7] Rozilah A, Aiza Jaafar C N, Sapuan S M, Zainol I and Ilyas R A 2020 The effects of silver nanoparticles compositions on the mechanical, physiochemical, antibacterial, and morphology properties of sugar palm starch biocomposites for antibacterial coating *Polymers (Basel)* **12** 1–21
[8] Hu X, Jia X, Zhi C, Jin Z and Miao M 2019 Improving the properties of starch-based antimicrobial composite films using ZnO-chitosan nanoparticles *Carbohydr Polym.* **210** 204–9
[9] Basumatary K, Daimary P, Das S K, Thapa M, Singh M, Mukherjee A and Kumar S 2018 Lagerstroemia speciosa fruit-mediated synthesis of silver nanoparticles and its application as filler in agar based nanocomposite films for antimicrobial food packaging *Food Packag Shelf Life* **17** 99–106
[10] Akhila P P, Sunooj K V, Navaf M, Aaliya B, Sudheesh C, Sasidharan A, Sabu S, Mir S A, George J and Mousavi Khaneghah A 2022 Application of innovative packaging technologies to manage fungi and mycotoxin contamination in agricultural products: current status, challenges, and perspectives *Toxicon* **214** 18–29
[11] Basumatary I B, Mukherjee A and Kumar S 2023 Chitosan-based composite films containing eugenol nanoemulsion, ZnO nanoparticles and Aloe vera gel for active food packaging *Int. J. Biol. Macromol.* **242** 1–11
[12] Liu T and Liu L 2020 Fabrication and characterization of chitosan nanoemulsions loading thymol or thyme essential oil for the preservation of refrigerated pork *Int. J. Biol. Macromol.* **162** 1509–15
[13] Sharma K, Munjal M, Sharma R K and Sharma M 2023 Thymol encapsulated chitosan-Aloe vera films for antimicrobial infection *Int. J. Biol. Macromol.* **235** 1–9
[14] Granata G, Stracquadanio S, Leonardi M, Napoli E, Malandrino G, Cafiso V, Stefani S and Geraci C 2021 Oregano and thyme essential oils encapsulated in chitosan nanoparticles as effective antimicrobial agents against foodborne pathogens *Molecules* **26** 1–14
[15] Homayonpour P, Jalali H, Shariatifar N and Amanlou M 2021 Effects of nano-chitosan coatings incorporating with free /nano-encapsulated cumin (Cuminum cyminum L.) essential oil on quality characteristics of sardine fillet *Int. J. Food Microbiol.* **341** 1–10

[16] Yadav V, Pal D and Poonia A K 2024 Nanofillers as a potential key for shaping the future of the industries *Hybrid Advances* **7** 1–9
[17] Tanaşă F, Nechifor M and Teacă C A 2024 Essential oils as alternative green broad-spectrum biocides *Plants* **13** 1–36
[18] Hajibonabi A, Yekani M, Sharifi S, Nahad J S, Dizaj S M and Memar M Y 2023 Antimicrobial activity of nanoformulations of carvacrol and thymol: new trend and applications *Open Nano* **13** 1–21
[19] Mukurumbira A R, Shellie R A, Keast R, Palombo E A and Jadhav S R 2022 Encapsulation of essential oils and their application in antimicrobial active packaging *Food Control* **136** 1–14
[20] Medina E, Caro N, Abugoch L, Gamboa A, Díaz-Dosque M and Tapia C 2019 Chitosan thymol nanoparticles improve the antimicrobial effect and the water vapour barrier of chitosan-quinoa protein films *J. Food Eng.* **240** 191–198
[21] Caro N, Medina E, Díaz-Dosque M, López L, Abugoch L and Tapia C 2016 Novel active packaging based on films of chitosan and chitosan/quinoa protein printed with chitosan-tripolyphosphate-thymol nanoparticles via thermal ink-jet printing *Food Hydrocoll* **52** 520–32
[22] Tan S X, Andriyana A, Ong H C, Lim S, Pang Y L and Ngoh G C 2022 A comprehensive review on the emerging roles of nanofillers and plasticizers towards sustainable starch-based bioplastic fabrication *Polymers (Basel)* **14** 1–27
[23] Taherimehr M, YousefniaPasha H, Tabatabaeekoloor R and Pesaranhajiabbas E 2021 Trends and challenges of biopolymer-based nanocomposites in food packaging *Compr. Rev. Food Sci. Food Saf.* **20** 5321–44
[24] Mohd Salahuddin M B, Nurain M J, Alifdalino S, Mohd Zuhair M N, Nor Nadiah A K S and Siti Hajar A 2020 Optimizing the processing factor and formulation of oat-based cookie dough for enhancement in *Processes* **8** (797) 1–19
[25] Mandić A K, Bečelić-Tomin M, Kerkez Đ, Milidrag G P, Pešić V and Prica M 2020 A mini review: optimal dye removal by fenton process catalysed with waste materials *International Symposium on Graphic Engineering and Design* 205–11 University of Novi Sad - Faculty of Technical Sciences, Department of Graphic Engineering and Design
[26] Bidari R, Abdillah A A, Ponce R A B and Charles A L 2023 Characterization of biodegradable films made from taro peel (Colocasia esculenta) Starch *Polymers (Basel)* **15** 1–17
[27] Sandhu K S, Sharma L, Kaur M and Kaur R 2020 Physical, structural and thermal properties of composite edible films prepared from pearl millet starch and carrageenan gum: Process optimization using response surface methodology *Int. J. Biol. Macromol.* **143** 704–13
[28] Niu X, Ma Q, Li S, Wang W, Ma Y, Zhao H, Sun J and Wang J 2021 Preparation and characterization of biodegradable composited films based on potato starch/glycerol/gelatin *J. Food Qual.* **2021** 1–11
[29] Amaba A S, Villanueva K C, Tan N P, Siacor F D and Paler M K 2023 Preparation of bioplastic film from chitosan and mango (Mangifera Indica L. Anacardiaceae) kernel starch by casting method *Applied Chemical Engineering* **6** 1–15
[30] Mittal M, Chaudhary R, Phutela K, Airon M and Singh R C 2022 Modeling and performance optimization of starch-based biocomposite films using response surface methodology *Journal of Applied Research and Technology* **20** 430–47
[31] Cirillo G, Spizzirri U G and Iemma F 2015 *Functional Polymers in Food Science* **1** 176–9
[32] Shapi'i R A, Othman S H, Naim M N and Tawakkal I S M A 2025 Effect of chitosan-thymol ratio on the encapsulation of thymol in chitosan nanoparticle *Colloids Surf. A Physicochem Eng. Asp* **721** 1–11
[33] Shapi'i R A, Othman S H, Nazli Naim M and Kadir Basha R 2020 Effect of initial concentration of chitosan on the particle size of chitosan nanoparticle *Int. J. Nanotechnol.* **16** 680–91
[34] ASTM D882-18 2018 *Standard Test Method for Tensile Properties of Thin Plastic Sheeting* (ASTM International)
[35] Mali S, Grossmann M V E, García M A, Martino M N and Zaritzky N E 2006 Effects of controlled storage on thermal, mechanical and barrier properties of plasticized films from different starch sources *J. Food Eng.* **75** 453–60
[36] Shapi'i R A, Othman S H, Naim M N and Kadir Basha R 2019 Mechanical properties of tapioca starch-based film incorporated with bulk chitosan and chitosan nanoparticle : a comparative study *Pertanika (Science and Technology)* **27** 95–107
[37] Mohsenabadi N, Rajaei A, Tabatabaei M and Mohsenifar A 2018 Physical and antimicrobial properties of starch-carboxy methyl cellulose film containing rosemary essential oils encapsulated in chitosan nanogel *Int. J. Biol. Macromol.* **112** 148–55
[38] Cruz-Tirado J P, Barros Ferreira R S, Lizárraga E, Tapia-Blácido D R, Silva N C C, Angelats-Silva L and Siche R 2020 Bioactive andean sweet potato starch-based foam incorporated with oregano or thyme essential oil *Food Packag Shelf Life* **23** 100457
[39] Sotelo-Boyas M, Correa-Pacheco Z, Bautista-Banos S and Gomez y Gomez Y 2017 Release study and inhibitory activity of thyme essential oil-loaded chitosan nanoparticles and nanocapsules against foodborne bacteria *Int. J. Biol. Macromol.* **103** 409–14
[40] Othman S H, Kechik N R A, Shapi R A, Talib R A and Tawakkal I S M A 2019 Water sorption and mechanical properties of starch/chitosan nanoparticle films *J. Nanomater.* **2019** 1–12
[41] Syafiq R M O, Sapuan S M, Zuhri M Y M, Othman S H and Ilyas R A 2022 Effect of plasticizers on the properties of sugar palm nanocellulose/cinnamon essential oil reinforced starch bionanocomposite films *Nanotechnol Rev.* **11** 423–37
[42] Minitab Support 20 November 2024 https://support.minitab.com/en-us/minitab/help-and-how-to/statistical-modeling/using-fitted-models/supporting-topics/response-optimization/what-are-individual-desirability-and-composite-desirability/